Experimental Study of the Flow Field Inside a Whirling Annular Seal

by

Gerald L. Morrison, Professor
Robert E. DeOtte, Jr., Research Engineer
H. Davis Thames III, Graduate Student

Presented At:

4th International Symposium on
Transport Phenomena and
Dynamics in Rotating Machinery

April 5-8, 1992
Honolulu, Hawaii

Experimental Study of the Flow Field
Inside a Whirling Annular Seal

Gerald L. Morrison, Professor
Robert E. DeOtte, Jr., Research Engineer
H. Davis Thames III, Graduate Student
Turbomachinery Laboratory
Mechanical Engineering Department
Texas A&M University
College Station, Texas 77843-3123

ABSTRACT

The flow field inside a whirling annular seal has been measured using a 3-D Laser Doppler Anemometer (LDA) system. The seal investigated has a clearance of 1.27 mm, a length of 37.3 mm and is mounted on a drive shaft with a 50% eccentricity ratio. This results in the rotor whirling at the same speed as the shaft rotation (whirl ratio = 1.0). The seal is operated at a Reynolds number of 12,000 and a Taylor number of 6,300 (3,600 rpm). The 3-D LDA system is equipped with a rotary encoding system which is used to produce phase averaged measurements of the entire mean velocity vector field and Reynolds stress tensor field from 0.13 mm upstream to 0.13 mm downstream of the seal. The mean velocity field reveals a highly three dimensional flow field with large radial velocities near the inlet of the seal as well as a recirculation zone on the rotor surface. The location of maximum mean axial velocity migrates from the pressure side of the rotor at the inlet to the suction side at the exit. Turbulence production is a maximum near the seal inlet as indicated by the rapid increase of the turbulence kinetic energy (κ). However, turbulence production and dissipation attain equilibrium fairly quickly with κ remaining relatively constant over the last half of the seal.

NOMENCLATURE

A = leakage area, πDc, m^2
c = nominal clearance between the rotor and stator = R2-R1, m
D = stator diameter, m
L = rotor length, m
Q = leakage rate, m^3/s
Re = Reynolds number = $2\rho Uc/\mu$
$R1$ = rotor radius, m
$R2$ = stator radius = D/2, m
Ta = Taylor number = $[\rho W_{sh}c/\mu][2c/D]^{1/2}$
U = average leakage velocity = Q/A, 3.71 m/s
U_x = axial mean velocity, m/s
U_r = radial mean velocity, m/s
U_θ = azimuthal mean velocity, m/s

$\overline{u'_x u'_x}$ =	axial time averaged Reynolds normal stress, m^2/s^2
$\overline{u'_r u'_r}$ =	radial time averaged Reynolds normal stress, m^2/s^2
$\overline{u'_\theta u'_\theta}$ =	azimuthal time averaged Reynolds normal stress, m^2/s^2
W_{sh} =	azimuthal velocity of the rotor surface, 30.9 m/s
X =	axial distance from seal inlet, m
θ =	azimuthal angle measured from the minimum clearance in the direction of shaft rotation, clockwise on the figures
κ =	turbulence kinetic energy = $\frac{1}{2}(\overline{u'_x u'_x} + \overline{u'_r u'_r} + \overline{u'_\theta u'_\theta})$, m^2/s^2
μ =	absolute viscosity of the fluid (water), Ns/m^2
ρ =	fluid density, Kg/m^2
( )' =	fluctuating value = instantaneous value - mean value
$(\overline{})$ =	mean value (time averaged)

INTRODUCTION

The influence of seals upon the rotordynamic stability of turbomachines has become an important concern in the last 20 years as turbomachines have become lighter and have been required to operate at increasingly higher speeds. This was clearly demonstrated on the Space Shuttle Main Engines (SSME) where the seals became a critical element in the stable operation of the turbomachine. Accurately predicting the leakage rate through a seal is an extremely difficult task due to the great number of geometric variables as well as harsh operating conditions and exotic fluids. Such complexity pushed the limits of empirical and bulk flow models. Now with the additional requirement of knowing the forces generated by the seal and how they effect the rotordynamic stability, a new generation of analyses is needed.

To address this challenge, Tam, Przekwas, Muszynska, Hendricks, Braun, and Mullen[1] undertook a numerical and analytical study of the fluid dynamic forces in seals and bearings. They solved the Reynolds averaged Navier-Stokes equations for the turbulent, swirling flow field inside annular seals using the PHOENICS-84 numerical code. In their study[1], the effects of preswirl, whirl ratio, overall pressure drop, shaft speed, fluid injection, and eccentricity ratio upon the flow field were examined and an evaluation of the resultant fluid dynamic forces generated by the seal was performed. These calculated forces and overall leakage rates were then compared with measurements performed by Childs[2,3]. Overall, good agreement was obtained.

OBJECTIVES

There is one obstacle standing in the way of further advancement of this type of computational analysis - the turbulence model. The statement of Tam, et.al.[1], "until fluctuation details for high shear flows at low clearances become available the simplest of the turbulence models was selected for the present calculations," indicates a need for more detailed basic information. In order to adequately evaluate the effectiveness of the turbulence model, details of the flow field (velocity field and the Reynolds stress tensor) are required. It is the objective of an ongoing research project at the Turbomachinery Laboratory, funded by NASA Lewis, to obtain this required data. Presented in this paper is a portion of the results. In particular, the distributions for the three mean velocity components and the turbulence kinetic energy level are presented for one axial location immediately upstream of the seal inlet and five axial positions along the length of the seal. Additional information, including the Reynolds stress tensor, was obtained at various other axial locations; space limitations, however, prohibit the presentation of all this information in one paper. The data are available on MS-DOS disks and a more complete presentation is available in Mr. H.D. Thames' thesis[4].

FACILITIES AND INSTRUMENTATION

The facility used in this investigation has been previously described in detail by Morrison[5,6]. Briefly, the test section (Figure 1) consists 50.4 mm diameter overhung shaft directly coupled to a 37 kW electric

induction motor. The electric motor is driven by a power supply capable of varying speeds from 200 to 5,300 rpm. The seal itself is composed of an acrylic rotor (0.164 m O.D.) and a stainless steel stator with a nominal clearance between the rotor and stator that is 1.27 mm. The rotor is optically coated by a vacuum-deposition technique to reduce reflected light intensity and is mounted on the stainless steel shaft using a brass bushing, the outer circumference of which is 0.63 mm eccentric with reference to the axis of the shaft. This results in the rotor being eccentric causing whirl in a circular orbit at the same speed as the shaft (whirl ratio 1.0). The seal stator is constructed of stainless steel with a smooth finish. To permit access for the LDA system, a flat optical window is installed in a narrow slit along the axis of the seal. A flat window is used to avoid lens effects. The deviation from roundness resulting from the window is only 1.5% of the clearance or 0.027% of the rotor radius. The annular seal is a constant radius design which is 37.3 mm long.

A 3.75 m^3 storage tank supplies water at approximately 300 K to a centrifugal pump. The pump flow rate of 0.00243 m^3/s is set by a throttling valve and metered by a turbine flow meter. After metering, the water is introduced into the seal rig and water exiting the seal is returned to the storage tank. Expansel 462 WU, 6 μm diameter plastic sphere with a specific gravity of 1.23, is added to the water to provide light scattering seed for the laser Doppler anemometer system. This particle will follow instantaneous flow fluctuations up to 44,000 Hz.

Morrison, et al [5,6] have previously discussed in detail the 3-D LDA system used and have presented an error analysis for the system. The LDA system is a three color, six beam arrangement with 8.5X beam expanders. Two colors measure orthogonal velocity components and the optical axis for the third color is inclined at 30° to the others. This results in a measurement volume 0.025 X 0.025 X 0.10 mm in size. Bragg cells are installed on one beam of each color pair so that flow reversals can be measured. This LDA system is thus capable of measuring the instantaneous 3-D velocity vector at the measurement volume. The data acquisition systems consists of a rotating machinery resolver and three counters which supply the angle of the rotor as well as the three non-orthogonal velocity components to an 80386 computer system. A gate on the master interface assures that all three counters measure a velocity component within a coincidence window of 10 μs. The data is then post processed to calculate the mean velocity, Reynolds stress tensor, and other quantities with the data divided into 20 different angular positions of the rotor, each with a window of 18° (one window had inadequate data for analysis). A minimum of 90,000 velocity realizations sorted into the different angular positions of the rotor were recorded at each X and r location. This resulted in a minimum of 1000 and a maximum of approximately 8000 samples at each reported location for a given phase window. Figure 2 presents the locations on the r-θ plane where the measurements were made.

Recent experience (Wiedner[7] and Morrison[8]) with this system has shown that there is some velocity bias present in the data which is best corrected using the McLaughlin-Tiederman[9] velocity bias correction technique. Uncertainties are estimated[5] to be ±1% on U_x and U_θ, ±2% on U_r, and 20% on κ.

RESULTS

Isovels were calculated from the data for the axial (U_x), radial (U_r), and azimuthal (U_θ) mean velocity components at X/L = -0.0018, 0.00, 0.21, 0.50, 0.77, and 1.00. Plots of these are presented in Figures 3-5. The rotor is orbiting in the clockwise direction (increasing θ).

The seal influences the mean velocity field immediately upstream (X/L = -0.018) of the inlet in two ways. First, because the large end of the rotor is exposed to the supply plenum, there is an induced preswirl which varies from 6% of the rotor surface speed (0.06W_{sh}, 0.50U) near the stator wall to 28% near the rotor. Secondly, the flow accelerates into the seal with the maximum axial velocity (1.3U) occurring near θ = 105° rather than at the maximum clearance location (θ = 180°). With the rotor spinning clockwise, it appears that fluid approaching the inlet at the region of maximum clearance maintains the axial momentum necessary to enter the seal but must accelerate as it is rotated into the smaller gap. This hypothesis is further substantiated in the analysis of the axial velocity contours at X/L = 0.00 where the fluid is semi-confined yet the precession of the rotor causes the axial velocity to increase even more (2.4U) as the clearance decreases ($\theta \approx 75°$). It is interesting that the fluid not only continues flowing downstream as the clearance decreases but actually experiences this substantial increase in local axial velocity. This is consistent with continuity since the azimuthal velocity remains small compared to the axial velocity at this azimuthal location. In this region, large outward radial velocities (0.9U) are caused by the rotor

moving toward the stator. In fact, the U_r-U_θ velocity vector in this plane is almost entirely in the outward radial direction for the rotor phase $30° \leq \theta \leq 180°$. This combined with the steep $\partial U_x/\partial r$ near the rotor indicate the presence or onset of a flow separation on the rotor (as evidenced by the close spacing of the contours).

On the opposite side of the rotor (the phase where the clearance is increasing, $\theta > 180°$), the mean axial velocity decreases as θ increases until there is a negative axial velocity component (flow from the seal back into the plenum) from $\theta = 270°$ to $350°$. The minimum velocity is -0.4U at X/L = -0.018 and -0.3U at X/L = 0.00. This side of the rotor ($180° < \theta < 360°$) is typically called the suction side. Therefore, one might expect this region where the clearance is increasing to provide less resistance to flow and to "suck in" fluid which would result in a positive U_x. However, in this case, a strong azimuthal velocity component, U_θ, is bringing fluid into the widening clearance at a faster rate than the expansion can support causing a pressure increase. This results in the fluid actually "squirting out" of the seal back into the inlet plenum.

Progressing from X/L = 0.00 to 0.21, the region of maximum U_x moves counter-clockwise to $\theta \approx 90°$ and outward radially while decreasing in maximum value from 2.4U to 1.5U. The region occupied by the high speed flow is more uniform with smaller $\partial U_x/\partial r$ gradients near the rotor indicating the reattachment of the flow to the rotor. U_x is positive across the entire cross-section with a minimum value of 0.2U, which indicates that a stagnation zone exists somewhere between X/L = 0.00 and 0.21. The radial velocities have become less than 10% of U compared to 80% at X/L = 0.00 indicating the flow is becoming more parallel to the stator. The azimuthal velocity distribution is much more uniform around the rotor being almost symmetric about $\theta = 0°$.

By the center of the seal, X/L = 0.50, U_x has been redistributed with the decreasing maximum velocity shifting clockwise. The flow is becoming established with the mean axial velocity being very nearly uniform over the entire seal and the radial velocity decreasing even further in amplitude to 0.04U. The azimuthal velocity distribution remains very much the same as at X/L = 0.21 except that there is a slight overall increase in magnitude.

The axial velocity component, U_x, continues to show development by actually rotating locations of maximum value (1.5U) to $\theta \approx 315°$, where the backflow existed in the inlet, and the minimum U_x (0.4U) occurring where the maximum was present at the inlet. The radial velocities have increased slightly with a longer cross section of the flow having +0.04U. In the transition from X/L = 0.21 to 0.77 the regions of positive and negative radial velocity have exchanged places. The azimuthal velocity has increased slightly since X/L = 0.50 attaining approximately 35% of the shaft speed for $\theta < 90°$ and 25% for $\theta > 200°$. The azimuthal velocity distribution is the driving mechanism for the change in location of maximum mean axial velocity. From X/L = 0.50 to the end of the seal, U_θ is consistently larger for $\theta < 180°$. This causes a migration of the fluid with the maximum U_x from $\theta \approx 75°$ at the inlet to $\theta \approx 315°$ at X/L = 0.77. This effect continues until the exit of the seal where U_x attains the maximum value of 1.9U and the minimum value of 0.3U. In the exit plane the radial velocities begin to rise in value as the flow begins to rearrange for the step change in area at the exit.

One of the variables calculated in most turbulence models is the turbulence kinetic energy ($\kappa = \frac{1}{2}\{\overline{u_x u_x} + \overline{u_r u_r} + \overline{u_\theta u_\theta}\}$). It is a good measure of the level of turbulence present in the seal. As mentioned earlier, we have measured the entire Reynolds stress tensor which is available in Thames[4]. The contours of κ presented in Figure 6 show that immediately upstream of the seal, the turbulence level is large with a maximum $\kappa = 0.4U^2$. This corresponds to a turbulence intensity which is approximately 50% of the average leakage velocity (U). This occurs near the rotor at $\theta = 270°$ where U_x is zero. Over the majority of the field, κ ranges from $0.2U^2$ to $0.3U^2$ (35% to 45% turbulence intensity), however, once the flow enters the seal, the turbulence kinetic energy increases rapidly in the region near the rotor where the mean flow appears to separate, and hence κ exceeds $0.8U^2$. This is consistent with the very large radial gradient of the mean axial velocity ($\partial U_x/\partial r$) which contributes to the production of turbulence. As the flow progresses further downstream the turbulence kinetic energy levels decrease to approximately $0.3U^2$ at X/L = 0.21 and $0.2U^2$ for $0.50 \leq$ X/L ≤ 1.00. This relatively gradual change is expected since the spatial gradients of the mean velocity are significantly smaller for x/L ≥ 0.21 hence the mechanism for turbulence production is reduced and turbulence dissipation begins to balance the turbulence production.

CONCLUSIONS

The flow field inside a whirling annular seal has been measured using a 3-D LDA system. The mean velocity field reveals a highly three dimensional flow field with large radial velocities near the inlet of the seal and a recirculation zone on the rotor surface. Near the inlet the mean axial velocity is very large on the pressure side of the rotor but by the downstream half of the seal, the region of high mean axial velocity has migrated to the suction side. Near the inlet, on the suction side of the rotor, there is a back flow into the plenum which is caused by the large azimuthal velocity moving large quantities of fluid into the region which then "spill over" into the plenum. The radial velocities steadily decrease in value as the flow progresses through the seal until the exit plane is reached at which point they increase abruptly, however, the magnitude is still significantly lower than at the inlet. The overall azimuthal velocity steadily increases from approximately $0.12W_{sh}$ at the inlet to $0.30W_{sh}$ at the exit. The flow over the seal inlet produces very large levels of turbulence kinetic energy. However, turbulence production and dissipation attain equilibrium fairly quickly and κ remains relative constant over the last half of the seal.

ACKNOWLEDGMENT

REFERENCES

1   Tam, L.T., Przekwas, A.J., Muszynska, A., Hendricks, R.C., Braun, M.J., and Mullen, R.L., "Numerical and Analytical Study of Fluid Dynamic Forces in Seals and Bearings," *Transaction of the ASME - Journal of Vibration, Acoustics, Stress, and Reliability in Design*, Vol. 110, July 1988, pp. 315-325.

2   Childs, D.W., Vance, J.M., and Hendricks, R.C., eds, *Rotordynamic Instability Problems in High Performance Turbomachinery*, Proceedings of the Workshop held at Texas A&M University; NASA CP-2238, 1982.

3   Childs, D.W., "SSME HPFTP Interstage Seals: Analysis and Experiments for Leakage and Reaction Force Coefficients," NASA Contract NAS8-33716. Turbomachinery Laboratories, Texas A&M University, February, 1983.

4   Thames, H.D., "Mean Flow and Turbulence Characteristics in Whirling Annular Seals", Master of Science Thesis, Texas A&M University, Mechanical Engineering Department, May 1992.

5   Morrison, G.L., Johnson, M.C., and Tatterson, G.B., "Three-Dimensional Laser Anemometer Measurements in an Annular Seal," *Transactions of the ASME - Journal of Tribology*, Vol 113, July 1991, pp. 421-427.

6   Morrison, G.L., Johnson, M.C., and Tatterson, G.B., "3-D Laser Anemometer Measurements in a Labyrinth Seal," *Transactions of the ASME - Journal of Engineering for Gas Turbines and Power*, Vol 113, January 1991, pp. 119-125.

7   Wiedner, B.G., "Experimental Investigation of Velocity Biasing in Laser Doppler Anemometry," Master of Science Thesis, Texas A&M University. Mechanical Engineering Department, December, 1988.

8   Morrison, G.L., DeOtte, R.E., Jr., Nail, G.H., and Panak, D.L., "Mean Velocity Field and Turbulence Characterization of the Flow in an Orifice Flow Meter," *Laser Anemometry, Advances and Applications*, Vol. 1, August 1991, pp. 1-10.

9   McLaughlin, D.K., and Tiederman, W.G., "Biasing Correction for Individual Realization of Laser Anemometer Measurements in Turbulent Flows," *Physics of Fluids*, Vol. 16, 1973, p. 2082.
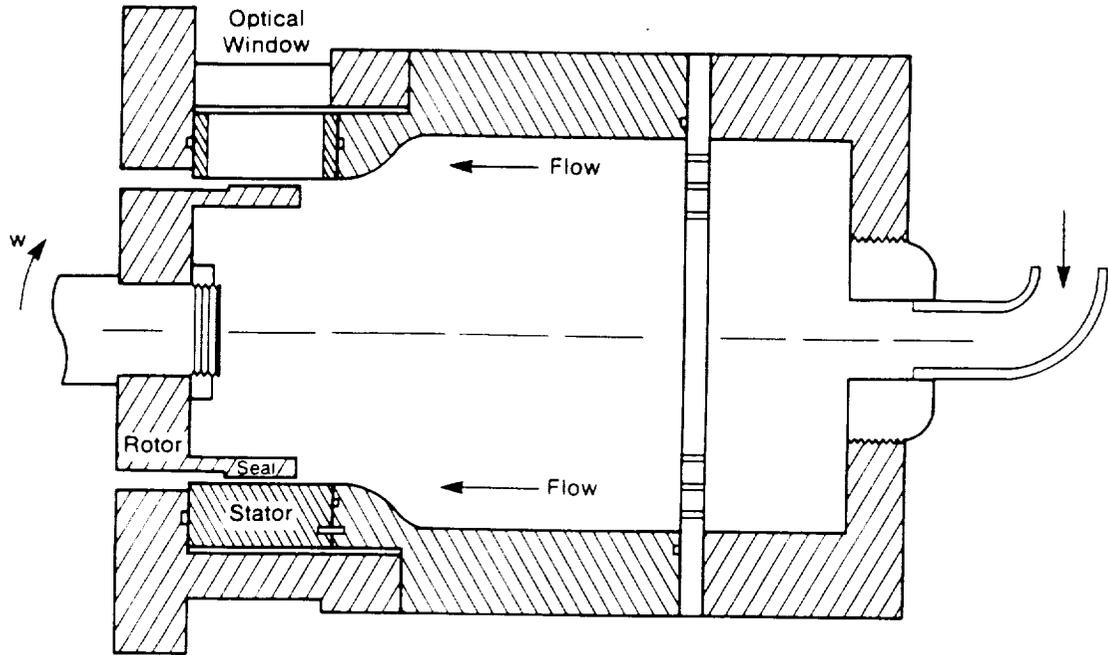
**Figure 1** Test Section
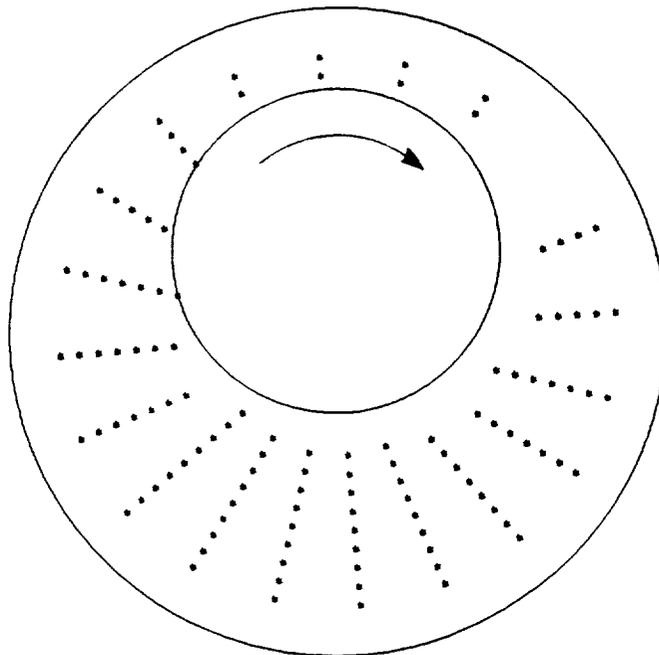
Figure 2 Measurement Grid

X/L = -0.018

X/L = 0.00

$\overline{U}_x/U$

$\overline{U}_r/U$

$\overline{U}_\theta/W_{sh}$
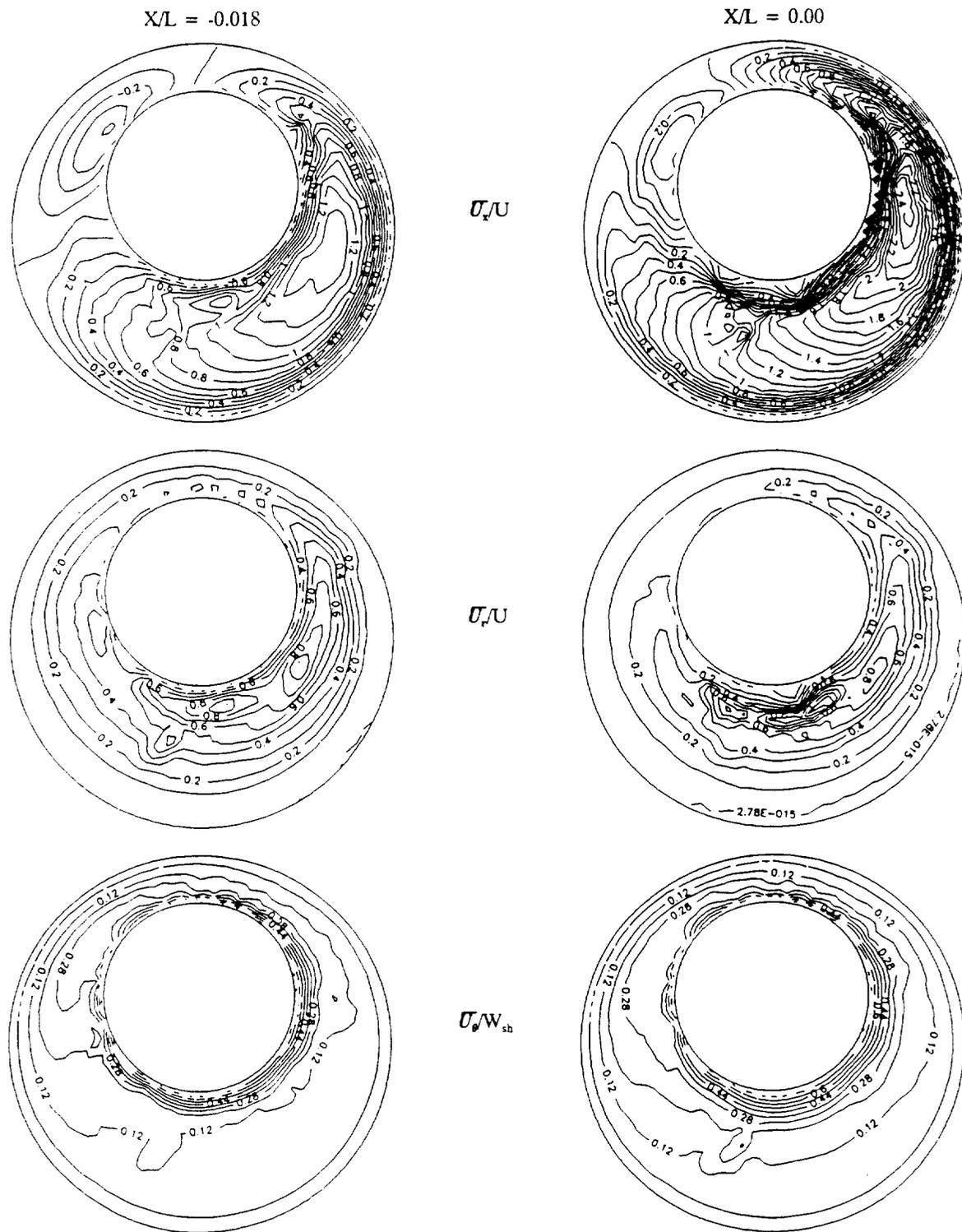
Figure 3 Mean Velocity Isovels, X/L = -0.018 and 0.00

X/L = 0.21   X/L = 0.50

$\overline{U}_x/U$

$\overline{U}_r/U$

$\overline{U}_\theta/W_{sh}$
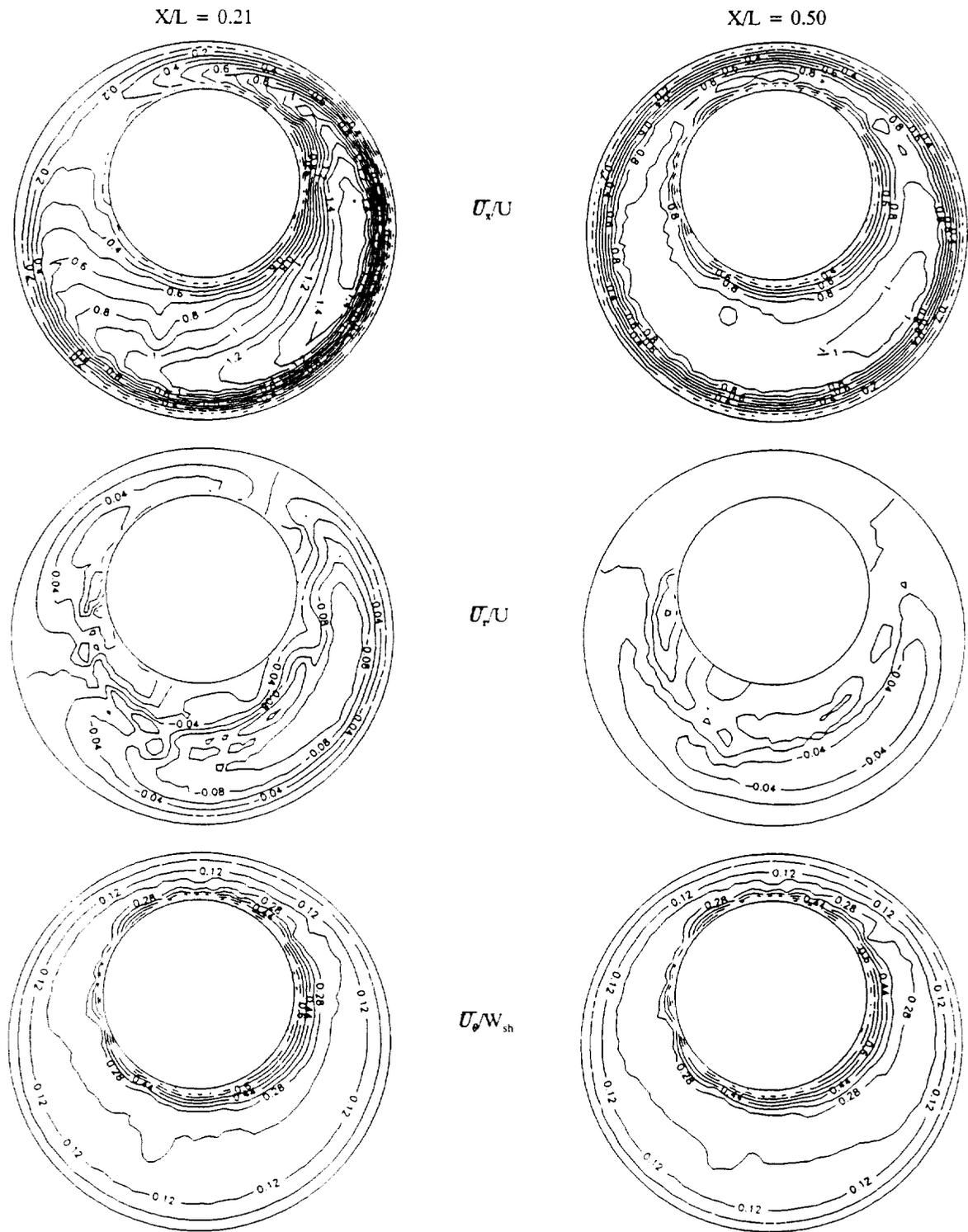
Figure 4 Mean Velocity Isovels, X/L = 0.21 and 0.50

X/L = 0.77   X/L = 1.00
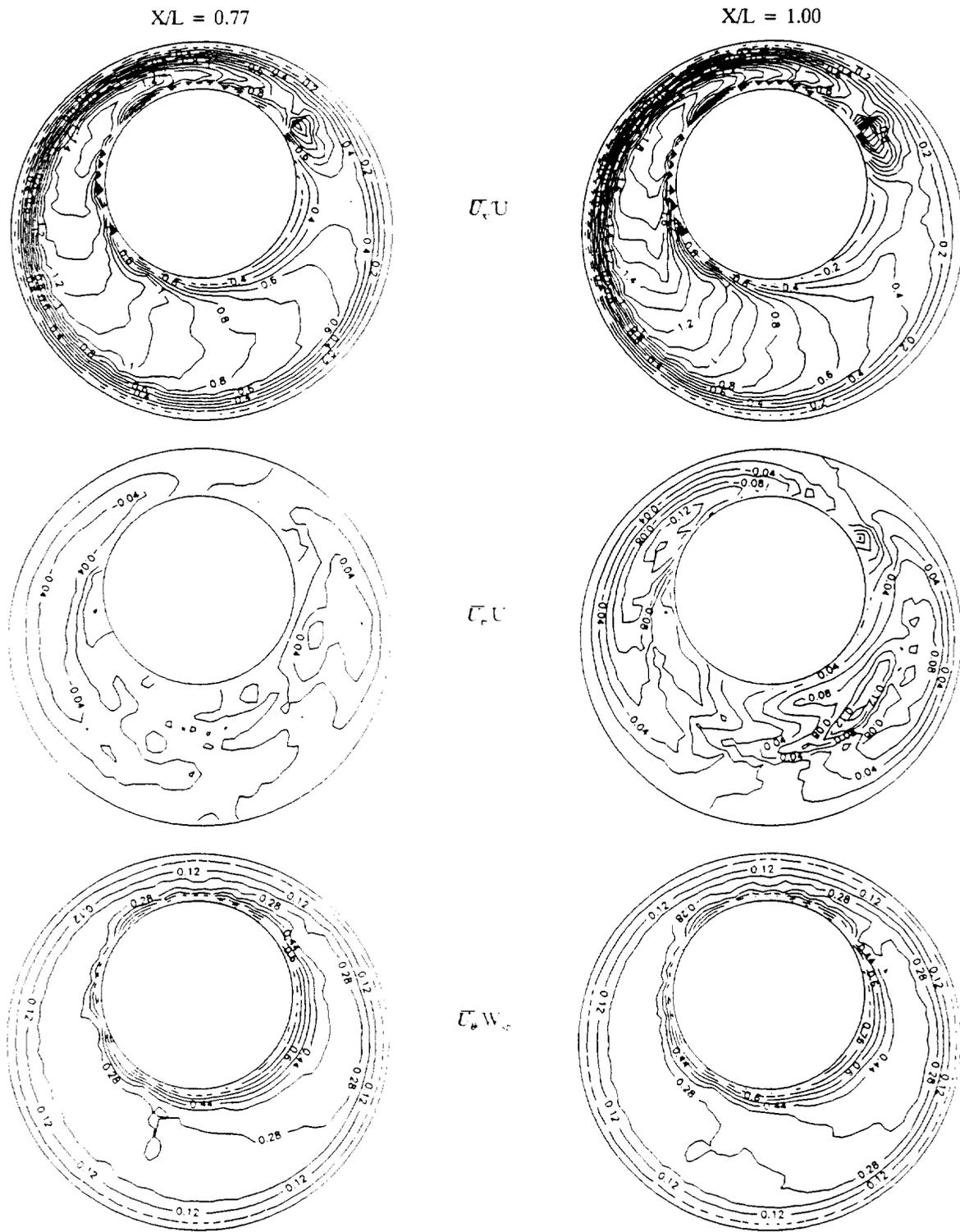
Figure 5   Mean Velocity Isovels. X/L = 0.77 and 1.00

X/L = -0.018

X/L = 0.00

X/L = 0.21

X/L = 0.50

X/L = 0.77

X/L = 1.00
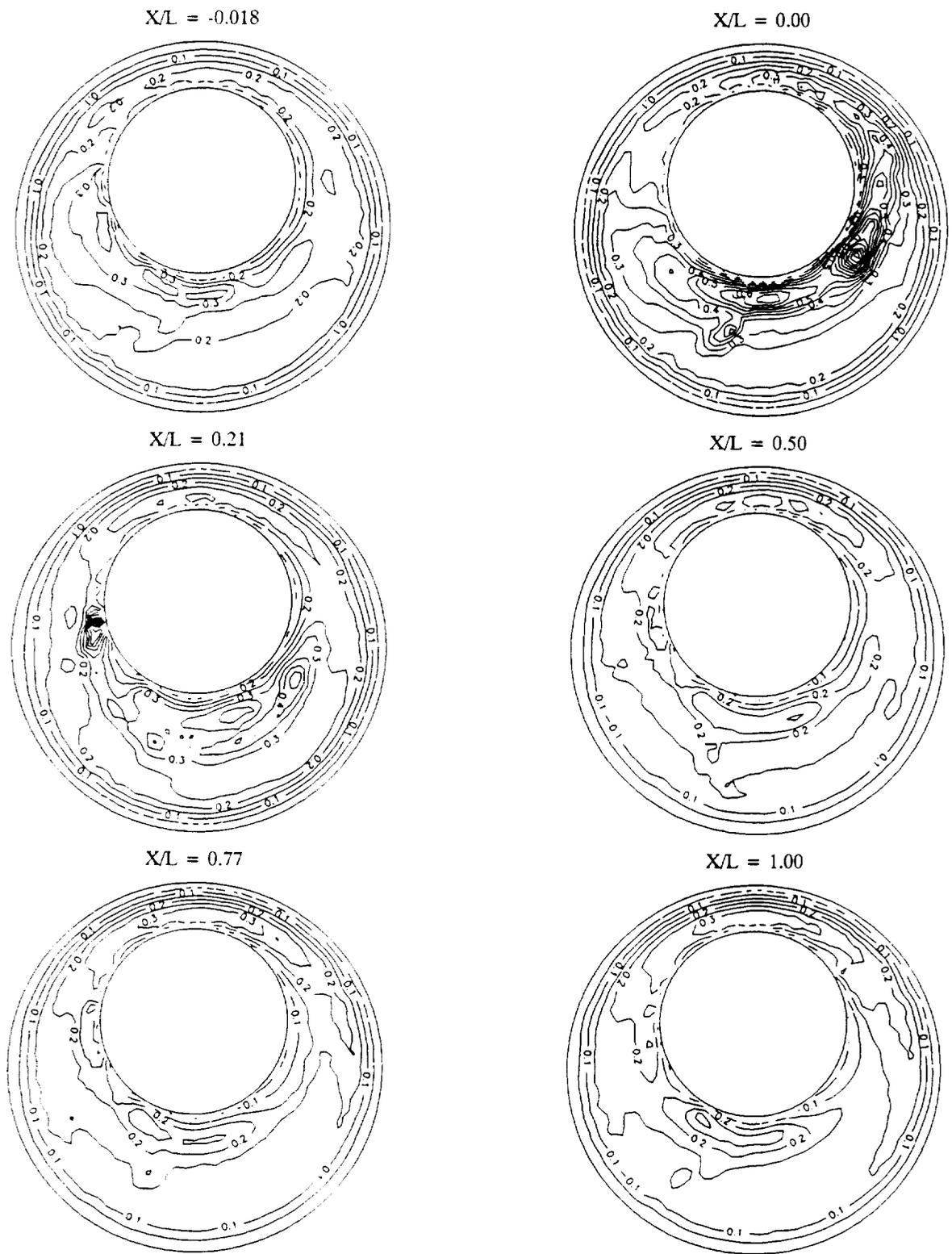
Figure 6 Turbulence Kinetic Energy, κ/U^2